Test-bed design and modeling for aircraft interior acoustic control

Michael L. R. Fripp and Donald Q. O'Sullivan
S. R. Hall, N. W. Hagood, K. Lilienkamp

Active Materials and Structure Laboratory
Department of Aeronautics and Astronautics
Massachusetts Institute of Technology
Cambridge, Massachusetts 02139

ABSTRACT

A cylindrical test-bed has been designed and modeled to aid in the study and control of interior acoustics in aircraft. The test-bed accounts for local as well as global structural-acoustic dynamics encountered in typical aircraft. The design is based on several existing aircraft and models used to study aircraft dynamics. The test-bed incorporates the basic geometry and materials common to a majority of aircraft, including an aluminum skin shrouding a framed structure composed of ribs and stringers. The design is approximately a one-third scale representation with a cylindrical geometry measuring 0.91 m diameter and 1.98 m long.

The test-bed has been modeled using finite element methods and Rayleigh-Ritz assumed modes analysis. The models were used to refine the design of the test-bed as well as to model the coupled structural-acoustic dynamics. The models predict that the test-bed will have a modal structure commensurate with experimental identifications on existing aircraft.

Keywords: structural-acoustic, test-bed, model, control, aircraft.

1. INTRODUCTION

The study and control of aircraft interior acoustics is an important avenue of research requiring new control techniques. Implementation on a representative test-bed is important for the validation of any new control system. Previous studies have investigated the noise transmission through flat panels[1-4] or through smooth cylinders[5]. More recent studies have investigated test-beds with more representative geometries and have placed reinforcing members on flat panels[6], have studied cylinders with ribs and stringers[7], or have examined actual aircraft fuselages[8-12]. This paper presents the design of a test-bed that is representative of the structural-acoustic dynamics encountered in rotorcraft and aircraft while sufficiently simplifying the structure to allow control research to be performed.

The emphasis of this research is placed on rotorcraft and aircraft interior acoustics due to the high sound pressure levels encountered. In general, commercial airplane interior sound pressure levels are considered barely tolerable for a working environment (~80 dB). Commercial helicopter sound pressure levels are much higher (~95 dB) and military helicopters are excessive (~115 dB).[13,14] Controlling aircraft interiors is challenging not only because of the higher noise levels, but also because of stringent space and weight requirements and the proximity of disturbance sources.[14] High decibel levels encountered in aircraft are annoying and can also cause human fatigue, inhibit motor skills, and lead to mechanical fatigue. Pilots usually wear headsets to block out excess noise, but headsets and other passive damping techniques principally attenuate high frequencies. Some of the most dangerous noise levels occur at low frequencies and are only weakly inhibited by passive damping.[12]

The test-bed is part of a program to investigate novel and computationally feasible methods of active structural feedback control for global quieting. For this end, the test-bed was designed to capture the dynamic characteristics of rotorcraft and aircraft. To facilitate test-bed control analysis, the design must be a simplified representation of a aircraft structure. The important characteristics that need to be represented in the test-bed are the global and panel structural dynamics, interior acoustic dynamics, and structural-acoustic coupling. Ideally the test-bed also should be constructed from commercially available components. The design that is presented in this paper balances this trade-off between realism and experimental necessity. Feedback control techniques will be experimentally validated on the test-bed in the next phase of the research. In designing the test-bed, realism of features that are most directly affected by the control design must be maintained. One

SPIE Vol. 3041 • 0277-786X/97/$10.00

significant feature is the panel design. A typical aircraft has hundreds of panels that couple well with the air and on which control potentially can be applied to achieve global interior quieting. One computationally feasible method to distribute control effort and achieve global quieting is to use a decentralized controller.[16-19] Even though the focus of this paper is experimental design and not control, it is important to recognize in the design process that the eventual purpose of the test-bed is for control.

This paper discusses the design and modeling of a structural-acoustic test-bed. This design is performed using a hybrid of geometric scaling and dynamic scaling techniques. Data from six aircraft related structures were collected in order to identify the key features of a fuselage. The test-bed was designed using hybrid scaling parameters in order to maintain the essential structural-acoustic dynamics. The test-bed was modeled using finite element methods and Rayleigh-Ritz analysis. The models were used to examine the coupled structural-acoustic dynamics and to design the end-cap geometry.

2. TEST-BED DESIGN METHODOLOGY

The design methodology provides for structured consideration of dynamic realism, structural simplification and design fabrication. This methodology is summarized in the flow chart in Figure 1.

2.1 Aircraft, rotorcraft and test-bed data

The primary aim in designing the test-bed was that it resemble the structural-acoustic dynamic characteristics of an actual fuselage. Exact reproduction of a particular fuselage's geometry or dynamics was not the design goal. Instead, the design was based on typical components from three aircraft and three aircraft models: Boeing Helicopters' CH-47D Chinook[20], Sikorsky S-70A Blackhawk[21], McDonnell-Douglas DC-9 test section[22], two NASA Langley Research Center structural-acoustic models[7], and a United Technologies Research Center (UTRC) structural-acoustic model[23]. Complete structural information was not available for the Blackhawk and the DC-9.

In general, many different frame sizes exist on a single fuselage. To aid in comparison, frame member geometry for each fuselage was averaged, while ensuring that the mass and stiffness properties were maintained. A similar process was applied to determine the average panel size for each of the fuselages. Table 1 outlines some of the geometric and structural properties of the six structures and their components.

2.2 Hybrid scaling

The simpliest test-bed design would feature a geometric scaling of the averaged aircraft structures. Unfortunately, geometric scaling not only would require components that are essentially unmanufactureable but also would require more panels than could be efficiently used in control design prototyping. As a result, a hybrid scaling which is a combination of geometric scaling and dynamic scaling is used to characterize the important features of the aircraft structures. The hybrid scaling parameters capture three main characteristics of the system dynamics: the global dynamics, the panel dynamics, and the relative dynamics between the frames and the panels.

Before the hybrid scaling parameters could be analyzed, the structures' sizes were normalized. The test-bed diameter was limited to 0.91 m due to anechoic facility constraints; hence, the aircraft structures and models were all geometrically scaled to this width. The structures' behavior was maintained as long as the frequency range of interest is scaled inversely with the characteristic length (frequency $\propto$ 1/characteristic length). With the structures normalized to the size of the test-bed, the data can be more easily compared. All of the scaling parameters will use the normalized aircraft data.

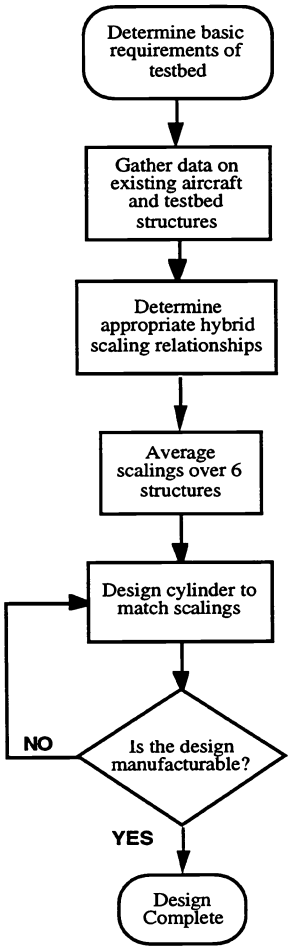

Figure 1: Flow chart of design methodology

Table 1: A comparison of unscaled geometric features for aircraft structures and models

Geometric features	*Boeing CH-47*	*Sikorsky Blackhawk*	*DC-9 section*	*Langley model 1*	*Langley model 2*	*UTRC model*
Length (m)	15.0	5.0	9.65	3.7	3.6	2.75
Width (m)	2.5	2.0	3.34	1.7	1.5	~1.65
Shape	Rounded box	Rounded box	Cylinder	Cylinder	Cylinder	Box
Panels:						
Circumferential number	10 to 25	NA	46	26	22	10
Thickness (mm)	0.5 - 1 Al	25 sandwich	1.6 Al	1.0 Al	0.81 Al	1.6 Al
Size (m)	0.76 x 1.0 to 0.31 x 0.51	NA x 0.84	0.23 x 0.48	0.20 x 0.38	0.21 x 0.33	0.61 x 0.76
Ribs:						
Total number	20	7	20	11	12	4
Bending inertia (m^4)	2.634×10^{-7}	3.2×10^{-6}	NA	2.88×10^{-8}	9.2×10^{-8}	3.06×10^{-6}
Torsional inertia (m^4)	2.97×10^{-7}	1.69×10^{-7}	NA	3.1408×10^{-8}	NA	6.12×10^{-6}
Area (m^2)	2.94×10^{-4}	4.43×10^{-4}	NA	7.23×10^{-5}	9.03×10^{-5}	3.95×10^{-3}
Stringers:						
Total number	15	NA	46	26	23	10
Bending inertia (m^4)	8.52×10^{-8}	NA	NA	1.94×10^{-9}	7.4×10^{-9}	0.372×10^{-6}
Torsional inertia (m^4)	7.87×10^{-8}	NA	NA	8.29×10^{-9}	NA	0.598×10^{-6}
Area (m^2)	5.61×10^{-4}	NA	NA	3.63×10^{-5}	7.09×10^{-5}	1.1×10^{-3}

To capture the global dynamics, the global structural stiffness was approximated from the structural properties by smoothing the ribs and stringers to create a constant thickness, thin walled cylinder. The global stiffness of a thin walled cylinder is dictated by the thickness. The smoothed cylinder thickness is found by using the mass per unit length for structures of the same radius and material. Table 2 lists the hybrid scaling parameters for the aircraft structures.

Since the high frequency modal behavior of the structures is dominated by the panels, it is necessary to characterize the panels separately. The first panel characteristic considered was the panel aspect ratio. The aspect ratio of the panel determines the modal ordering and frequency spacing of the panel modes. Another significant attribute of the panel is the relation of panel frequency to acoustic cavity frequency. This frequency ratio loosely represents the coupling behavior between the structural and acoustic disturbances and was derived by comparing the first panel mode to the first acoustic mode. For a flat panel the frequency ratio, FR_f, is

$$FR_f = \frac{\pi R}{2c}\left(\frac{1}{L^2}+\frac{1}{W^2}\right)\sqrt{\frac{Eh^2}{12\rho_p\left(1-\nu^2\right)}} \propto \frac{Rh}{L^2} \tag{1}$$

where c is the speed of sound in air, W is the panel width, E is the modulus of elasticity, ν is Poisson's ratio, ρ_p is the density of the panel material, R is the characteristic length of the acoustic structure, L is the characteristic length of the panel, and h is the thickness of the panel. For a curved panel an extra stiffening term must be included.[24] The frequency ratio for a curved panel, FR_c, is

$$FR_c = \frac{R}{2\pi c}\sqrt{\pi^4\left(\frac{1}{L^2}+\frac{1}{W^2}\right)^2\frac{Eh^2}{12\rho_p\left(1-\nu^2\right)}+\frac{EW^4}{\left(W^2+L^2\right)^2R^2\rho_p}} \tag{2}$$

In addition to characterizing the aspect ratio and frequency ratio, a third method was used to describe panel behavior by determining the mass ratio of the panel to a surrounding characteristic volume of air. This parameter helps maintain the proper structural-acoustic coupling between the panel and the air. The panel mass parameter, *MR*, is represented as

$$MR = \frac{\rho_p L^2 h}{\rho_a L^3} = \frac{\rho_p h}{\rho_a L} \tag{3}$$

where ρ_a is the density of air. For panels of the same density, the mass ratio is simply an expression of geometric scaling.

Note that all of the panel hybrid scaling parameters will not be matched unless the test-bed is geometrically scaled from the aircraft. Since geometric scaling is unfeasible, this indicates that the hybrid scaling technique is not exact. However, this technique provides a means of accounting and balancing opposing goals in designing the test-bed. As will be shown in the test-bed design in Section 3, the design allows for these scaling parameters to be nearly matched. This result is partially an artifact of the increased stiffness that resulted from the panel curvature.

The frame members of the structures required proper characterization. The purpose of aircraft frame members is to add both local and global stiffness to the structure. Since the total number of frame members in the test-bed will be different than in any of the structures, the total stiffness of the global frame stiffness is characterized by the sum of the bending inertias and the sum of the torsional inertias. A simple interpretation of frame inertia parameters is that if the number of stringers is cut in half the remaining stringers must have double the bending and rotational stiffness. Thus, as the size of the panels increases the frame members' stiffness and cross-sectional area increases and the number of frame members decreases. This metric maintains the relative deflection between the panels and frame members. The cross-sectional area of the frames was previously incorporated in the smoothed cylinder thickness used to calculate the global dynamics.

Two other aspects of the test-bed design required special consideration. The first consideration was the design of the test-bed ends. The nose and tail sections of actual aircraft are typically complicated non-regular structures. To contain cost and avoid actuator placement on the ends of the structure, a simplified end-cap was designed. The geometry of the end-cap was chosen to minimize the coupling, both structurally and acoustically, and, thus, was designed to be as rigid as possible. To meet these requirements the end-cap will be a 30° spherical section, which is stiffer and more massive than the frame and skin portion of the fuselage. Optimizing the end-cap design under these restrictions was accomplished with a finite element model. Both the design and the model are discussed in section 4.1.

The second consideration involved the application and spacing of fasteners. The fastener spacing was geometrically scaled with the rest of the aircraft parameters which roughly translates to a one centimeter spacing on the test-bed. This spacing rigidly attaches the panels to the frame and coincidentally puts the inter-fastener dynamics outside the frequency range of interest (>9000 Hz), since the spacing is less than a quarter wavelength of the highest frequency of interest. The fasteners must also maintain the mass of the structure and, hence, will be made of aluminum.

Table 2: A comparison of hybrid scaling parameters for aircraft structures and models

Hybrid scaling parameters (normalized)	*Boeing CH-47*	*Sikorsky Blackhawk*	*DC-9 section*	*Langley model 1*	*Langley model 2*	*UTRC model*
Mass per length (Kg/m)	3.65	NA	~5.5	4.43	4.06	37
Length/radius	12	5	5.8	4.3	4.8	3
Panel aspect ratio	1.34	NA	2.11	1.87	1.56	1.25
1st panel frequency/1st acoustic frequency	0.81	NA	0.52	0.44	0.55	0.04
Panel mass/Mass air volume	1.2	NA	4.5	3.5	3.0	7.7
Total rib bending inertia (m^4)	9.4×10^{-8}	9.3×10^{-7}	NA	2.5×10^{-8}	1.4×10^{-7}	1.6×10^{-6}
Total rib torsional inertia (m^4)	1.1×10^{-7}	4.9×10^{-8}	NA	2.8×10^{-8}	NA	NA
Total stringer bending inertia (m^4)	2.3×10^{-8}	NA	NA	4.4×10^{-9}	2.4×10^{-8}	4.8×10^{-7}
Total stringer torsional inertia (m^4)	2.1×10^{-8}	NA	NA	1.9×10^{-8}	5.7×10^{-8}	NA

Table 3: Experimental test-bed geometry and parameters compared to average structures investigated

Test-bed geometry and parameters	*Target design (normalized)* †	*Test-bed design*
Mass per length (Kg/m)	4.05	6.97 (w/o end-caps)
Length/radius	5.8	4.35
Panel aspect ratio	1.6	1.27
1st panel frequency/1st acoustic frequency	0.47	0.57
Panel mass/characteristic air volume	3.03	2.80
Total rib bending inertia (m^4)	8.63×10^{-8}	7.14×10^{-8}
Total rib torsional inertia (m^4)	6.23×10^{-8}	8.28×10^{-8}
Total stringer bending inertia (m^4)	1.71×10^{-8}	2.64×10^{-8}
Total stringer torsional inertia (m^4)	3.23×10^{-8}	5.24×10^{-8}

† Note: The averages for the rib and stringer inertia in table 3 do not include the UTRC model due to its lack of relation to the other aircraft in the study.

3. TEST-BED DESIGN

The following section presents the test-bed design, describes the geometric features, and compares the hybrid scaling parameters of the test-bed to those of the aircraft and aircraft model structures. The test-bed design meets the requirements of the research objective. The design is physically simplistic but includes modal complexity similar to that of a fuselage (see Sections 4.3). The test-bed incorporates control obstacles unique to a fuselage structure by representing the frame and skin construction. The test-bed is largely comprised of commercially available components which reduces manufacturing costs and simplifies assembly. Another feature of the test-bed is that panels can be cut out at a later time and replaced with adaptive composite panels. Table 3 lists some of the test-bed's geometric features as well as some of the hybrid scaling parameters. The table also compares the test-bed parameters with that of the geometrically scaled down (or normalized) average of the base structures.

As stated previously, the frame members are commercially available beams. Figure 2 relays their geometry and dimensions as well as the manner in which they will be fastened. It should be noted that the stringers in figure 2 will be modified from commercially available T-sections that are 2.54 cm by 2.54 cm. All other frame members are represented without modification. An estimated 4,300 separate fasteners will be required to assemble the test-bed. All skin sections will be permanently fastened while the end-caps will have removable fasteners to allow for interior access.

Figure 3 is a schematic of the actual test-bed design. The figure shows the test-bed half covered with skin so that the frame structure is visible. The basic dimensions of the test-bed are 91 cm in diameter and 198 cm in length. The test-bed is comprised of a total of 60 panels and incorporates twelve stringers and six ribs. The panel dimensions are 23.9 cm by 30.5 cm. The test-bed is manufactured from commercially available components, except for the end-caps which will be cold formed using a spinning process. The ribs are comprised of C-sections and the stringers are comprised of T-sections. The end-ribs are larger L-sections which attach to the flange of the end-caps. Fastening of the skin to the frame members will

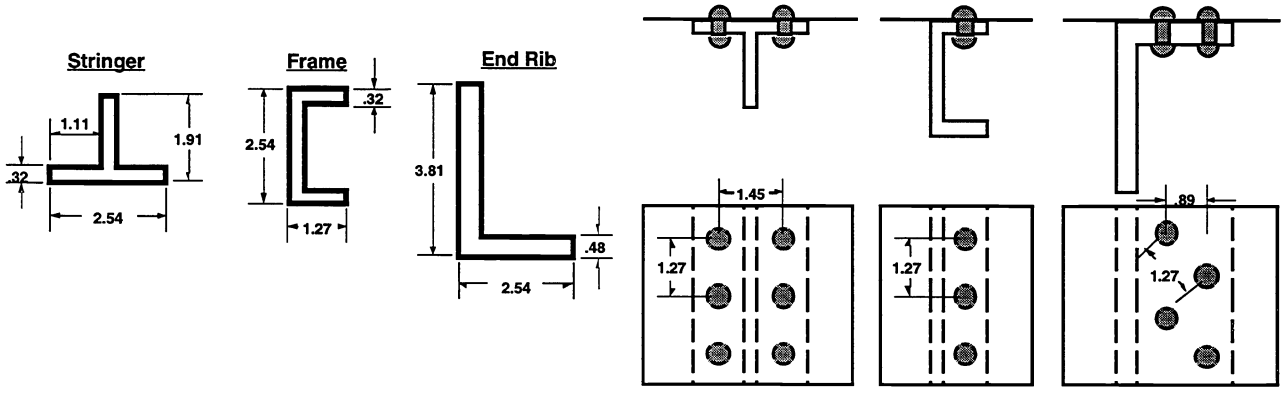

Figure 2: Schematic of frame member cross sections and fastener spacing and layout. All units in cm.

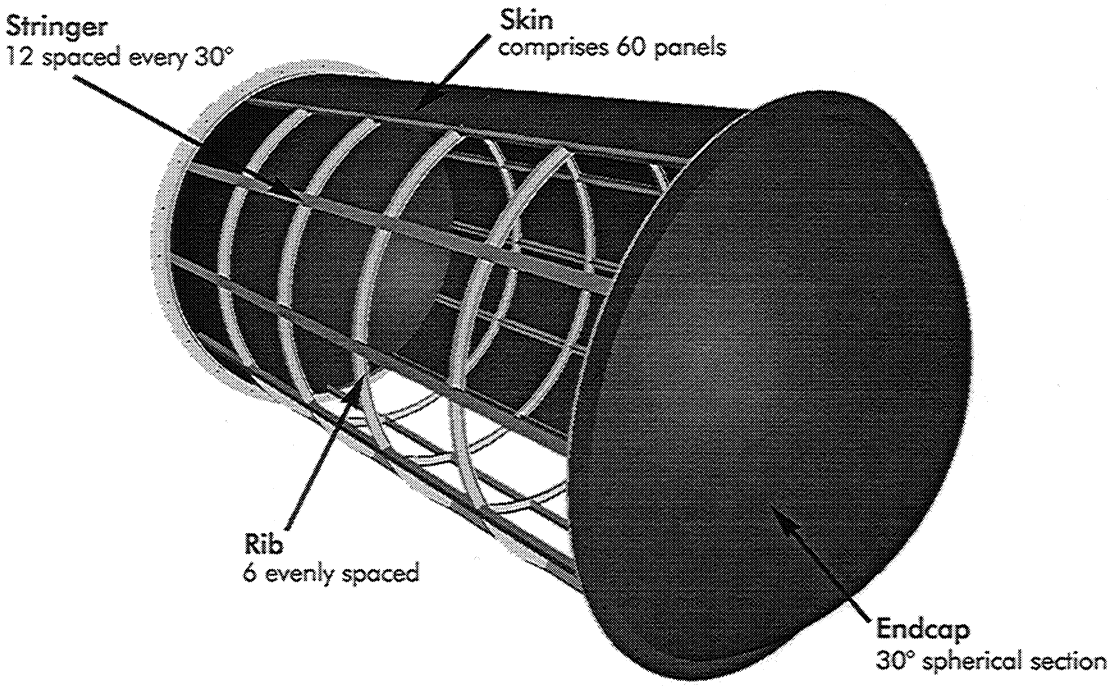

Figure 3: CAD rendition of experimental test-bed. Test-bed measures 0.91 m in diameter and 1.28 m in length

involve the use of rivets or welds spaced approximately every centimeter. The ribs will also be rigidly fastened to the stringers at intersections with spot welds. The skin is aluminum sheet 0.762 mm in thickness and is applied in four ninety degree sections with the seems running down the length of the stringers. The material is 6061 Aluminum alloy. Aluminum construction was used to minimize cost and to match the scaling parameters. The aluminum skin sections can be removed to perform tests on a composite skin.

4. MODELING

Computer models were created to help understand the dynamics and to help refine the design of the structural-acoustic test-bed. The models later will be used to optimize the actuator and sensor placement and also will form the basis for the control design. Two models of the test-bed were constructed: a finite element model and a Rayleigh-Ritz model. The finite element model was used to predict the coupled dynamics of the test-bed and to design the end-caps. The Rayleigh-Ritz model was used to corroborate the finite element model and to provide further insight into the coupled dynamics.

4.1 Finite element model

A finite element model of the frame reinforced cylinder, the cylinder end-caps, and the enclosed air was constructed using ANSYS 5.2. The cylinder skin and end-caps were assembled using curved shell elements, the ribs and stringers were assembled from beam elements, and the air was assembled from symmetric and un-symmetric fluid elements. Symmetric half models and quarter models of the test-bed were analyzed. A symmetric half model of the cylinder was used to design the end-caps. A symmetric quarter model of the test-bed was used to analyze the dynamics of the test-bed Only symmetric cases were considered which means that asymmetric modes were not captured. The element mesh of the finite element model is shown in figure 4.

A four element by four element mesh size was used on the panels . This grid size allowed the representation of panel modes up to 1500 Hz with 10% accuracy in the modal natural frequency. The first two modes were represented with a 5% accuracy in the natural frequencies. The modal accuracy was determined by calculating the natural frequency of a simply supported curved panel with varying mesh sizes. As the mesh size decreased, the accuracy of the natural frequencies increased. The percent modal accuracy is the percent difference between the natural frequency of the four element by four element mesh and a

thirty element by thirty element mesh. A four element by four element mesh size which was chosen as a balance between the accuracy of the modal natural frequencies and the time to arrive at a solution. The chosen mesh size resulted in 240 shell elements for the skin, 132 beam elements for the frame, and 450 fluid elements for the air in the quarter model of the test-bed. This combination of elements translates to roughly 5800 active degrees of freedom.

Modal analysis was performed using a symmetric quarter cylinder model. The quarter model is the exploded section in figure 4. The modal natural frequencies below 1 kHz were calculated for the structure, the enclosed air, and the coupled system and are presented in figure 5. Again, this only represents the symmetric modes.

The test-bed is modally dense. There are 63 structural modes, 42 acoustic modes, and 49 coupled structural-acoustic modes below 1 kHz in the quarter model. The structural modes occur in the same frequency range as the acoustic modes. The coupled modes occur at frequencies that are a combination of the structural modes and the acoustic modes. The cluster of structural and coupled modes near 400 Hz consists of modes whose nodal line aligns with the ribs but have different circumferential mode numbers. The modal density and modal frequency range of the test-bed are consistent with the modal density and modal frequency range experimentally identified in a DC-9 section[7].

The mode shapes of the first and eleventh coupled structural-acoustic mode of the test-bed are plotted in figure 6. These mode shapes represent the lowest frequency global mode and the lowest frequency panel mode. The first coupled mode is also the first structural mode and features the global dynamics of the test-bed. The eleventh mode is the first mode to feature significant panel deflection and is the lowest mode in the cluster of modes between 380 Hz and 430 Hz.

The finite element code also was used to design the end-cap geometry. As described in section 2.2, the end-caps should have minimal coupling with the interior acoustics and with the cylinder structure. Several end-cap geometries were modeled: flat, ellipsoidal, conic, hemispherical, and a shallow spherical section. The flat, ellipsoidal, and conic end-caps strongly couple with the interior acoustics. A hemispherical end-cap has small coupling with the interior acoustics but couples strongly with the structural dynamics of the cylinder. The shallow spherical section not only minimizes the coupling with the interior acoustics but also minimizes radial deflections during structural excitation. Deflections of the spherical section were twenty-two times smaller than the deflections of the flat plate. The shallow spherical section also minimizes the size of the test-bed.

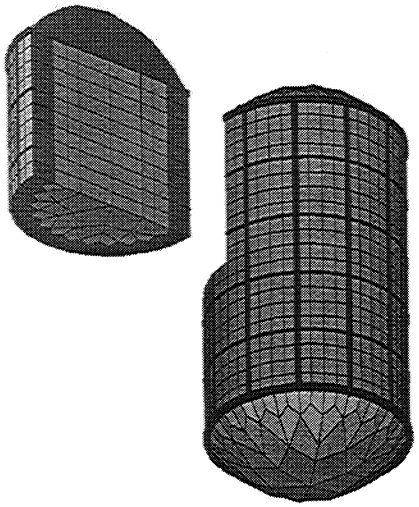

Figure 4: Finite element mesh of the test-bed. A symmetric quarter model (exploded section) was analyzed.

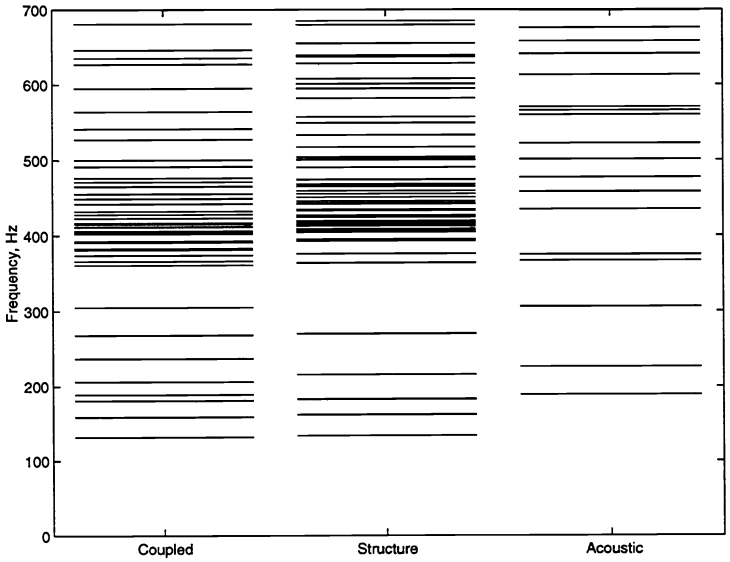

Figure 5: Natural frequencies of the quarter model test-bed calculated with finite element methods.

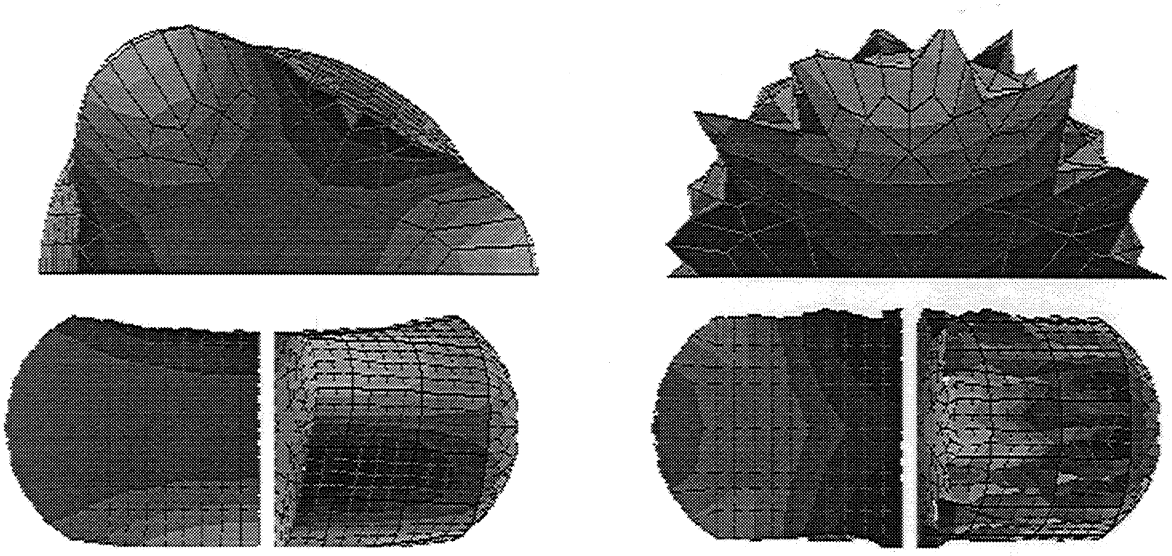

Figure 6: First and eleventh coupled structural-acoustic mode shape of the quarter-model test-bed calculated by finite element analysis.

4.2 Rayleigh-Ritz model

A Rayleigh-Ritz model of the cylinder was created in order to further understand the dynamics of the test-bed. The Rayleigh-Ritz model includes the ribs and stringers on the cylinder but does not include the end-caps. Simply-supported end conditions were used at the end of the cylinder. The structural dynamics were coupled with the interior acoustics to produce a coupled analysis of the test-bed.

The Rayleigh-Ritz assumed mode analysis was used to numerically solve the coupled equations of motion for the test-bed dynamics. The structural equations of motion are based on the three-dimensional displacement Flügge's thin shell equations.[25] Three-dimensional analysis is important in order to describe the stretching as well as the bending of the curved shell. The shape functions for the structural dynamics of the reinforced cylinder were taken from the mode shapes of a simply supported smooth cylinder:

$$U_m(x,\theta) = \cos\left(j\pi\frac{x}{L}\right)\begin{Bmatrix}\cos(i\theta)\\ \sin(i\theta)\end{Bmatrix} \quad V_m(x,\theta) = \sin\left(j\pi\frac{x}{L}\right)\begin{Bmatrix}\sin(i\theta)\\ \cos(i\theta)\end{Bmatrix} \quad W_m(x,\theta) = \sin\left(j\pi\frac{x}{L}\right)\begin{Bmatrix}\cos(i\theta)\\ \sin(i\theta)\end{Bmatrix} \tag{4}$$

In the representation of the structural shape functions, j dictates the number of longitudinal modes and ranges from 1 to 5. Modes corresponding to j=5 will have nodal lines that align with the ribs. The circumferential mode number is given by i and ranges from 1 to 13. Modes corresponding to i=6,12 will have nodal lines that align with the stringers. As a result, the first panel mode of the test-bed corresponds to j=5, i=6. The Rayleigh-Ritz model incorporates 405 structural shape functions.

The acoustic equations of motion are the standard acoustic Helmholtz wave equations for the pressure variation.[26] The acoustic shape functions were taken from the mode shapes of a right circular hard-walled cylinder:

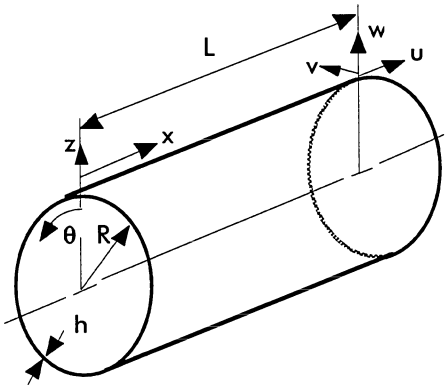

Figure 7: Cylinder coordinates

$$P_m(x,r,\theta) = J_j\left(\lambda_{jk}\frac{r}{R}\right)\cos(j\theta)\begin{Bmatrix}\cos\left(i\pi\frac{x}{L}\right)\\ \sin\left(i\pi\frac{x}{L}\right)\end{Bmatrix} \tag{5}$$

where J_i is the Bessel function of the first kind and i order, and λ is defined when the gradient of the pressure or acoustic velocity at the wall is zero. In the representation of the acoustic shape functions, i indicates the longitudinal mode number and ranges from 1 to 5, j indicates the circumferential mode number ranges from 0 to 13, and k indicates the radial mode number and ranges from 0 to 2. This resulted in 525 acoustic shape functions.

The structural natural frequencies for a simply-supported cylinder without air and without end-caps were calculated using the Rayleigh-Ritz assumed modes technique. The structural modal frequencies are plotted in figure 8 as a function of the number of circumferential modes. The out-of-plane deflections of the test-bed are a combination of stretching and bending. Modes with small circumferential mode numbers are dominated by stretching of the shell while modes with large circumferential mode numbers are dominated by bending. The lowest modal frequency occurs at the crossover between stretching and bending. As a result, the lowest natural frequency does not coincide with the mode that has the lowest circumferential mode number. For modes featuring significant rib deflection, the lowest natural frequency occurs at the third circumferential mode; this mode is illustrated in Figure 6 for the finite element solution.

At low circumferential mode numbers, the ribs and stringers add more mass than stiffness and, hence, slightly lower the modal natural frequencies. The natural frequencies are a strong function of the number of longitudinal variations at low circumferential mode numbers. At higher circumferential modes, circumferential bending dominates; frequency of modes with different number of longitudinal variations converge except for the fifth longitudinal mode. The fifth longitudinal mode does not produce bending in the ribs and, hence, occurs at a much lower frequency at high circumferential mode numbers. Concurrently, the lowest natural frequency of the fifth longitudinal mode occurs at the twelfth circumferential mode.

The sixth and twelfth circumferential modes have two frequencies because one mode aligns with the panels while the higher frequency orthogonal mode aligns with the stringers. The first panel mode of the test-bed corresponds to the fifth longitudinal mode and to the sixth circumferential mode.

The first twelve natural frequencies of the Rayleigh-Ritz mode are presented in table 4 as well as their corresponding finite element modal frequencies. For the first twelve Rayleigh-Ritz modes, the coupled dynamics of the two systems are similar. The frequency difference between the two systems is on the order of the 5%-10% frequency resolution of the finite element mesh size. Higher modes could not be correlated because the mode shapes found by one solution technique could not be identified from the modes found by the other solution technique. The first and fifth Rayleigh-Ritz mode are anti-symmetric modes and, thus, are not represented in the symmetric quarter model finite element solutions. Similarly, the fourth and fifth and the seventh and eigth Rayleigh-Ritz mode shapes are ninety degree rotations and, hence, only one of the pairs of modes are captured in the finite elements. Several of the lower frequency finite element mode shapes were not captured in the Rayleigh-Ritz solution because they feature interactions with the end-caps. The third and fifth finite element modes are predominantly acoustic modes whose mode

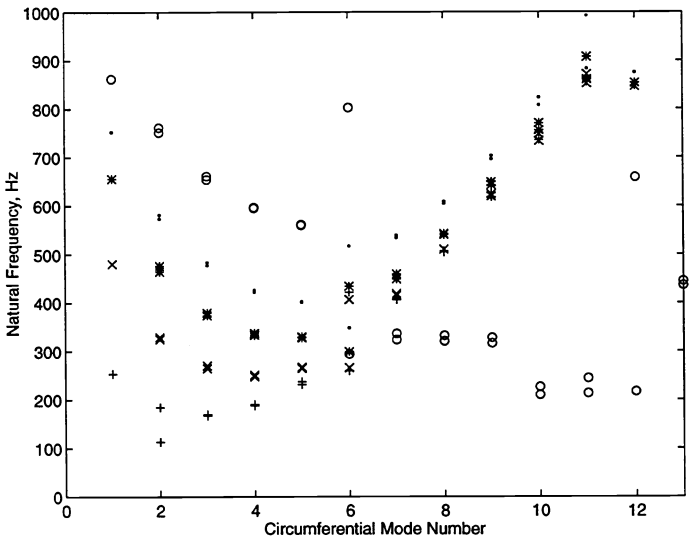

Figure 8: Natural frequencies of the test-bed without end-caps and without air, calculated by Rayleigh-Ritz method. Legend: Number of longitudinal variations: + - 1, x - 2, * - 3, . - 4, o - 5

Table 4: Coupled modal frequencies calculated by finite element methods and by Rayleigh-Ritz technique

Ritz Mode Number	*Ritz Frequency (Hz)*	*FEM Mode Number*	*FEM Frequency (Hz)*	*Percent Difference*
1	95	-	-	
2	138	1	131	+ 5%
3	190	4	189	+ 1%
4	259	6	237	+ 9%
5	261	6	237	+ 9%
6	284	-	-	
7	316	12	381	-17&
8	318	12	381	-17%
9	356	8	306	+16%
10	371	9	362	+ 2%
11	376	11	374	+ 1%
12	379	10	367	+ 3%

shapes are distorted due to reflections from the curved end-cap, and, hence, are not represented by the right circular Rayleigh-Ritz model.

4.3 Model correlation

The rib and stringer stiffened cylinder is a complicated structure. Small changes in the test-bed geometry have a strong effect on the natural frequencies of the system, especially since the system is being modeled over hundreds of modes. Small differences in the modeling technique cascade. Coupled structural-acoustic systems are modally dense and this density requires high modeling resolution. Close correlation between model and test-bed will require experimental updating of the model.[27]

The high modal density was a goal of the test-bed design. Actual aircraft are modally dense and the test-bed maintains the modal complexity. Additionally, aircraft have the structural modes and the acoustic modes in the same frequency region, which, again, the test-bed maintains. Finally, the modal frequencies of the test-bed are in the same region as the modal frequencies of a geometrically-scaled DC-9.[22] Although the test-bed does not exactly represent an aircraft, it does represent the dynamic complexity of a large class of aircraft.

5. SUMMARY AND FUTURE WORK

A methodology for designing a test-bed to study aircraft interior structural-acoustics has been presented. Using this methodology a representative test-bed was designed and modeled. The structural-acoustic dynamics of the test-bed match those of an actual aircraft fuselage. This verification was performed via finite element and Rayleigh-Ritz modeling. The test-bed structure was shown to have a modally dense behavior over the expected frequency ranges. Large global deflections occur below 380 Hz, while more complicated panel-influenced behavior dominate the higher frequencies.

The test-bed will provide insight into the dynamics of a fuselage and how to control undesirable dynamics. The simplifications made on the test-bed make for more feasible analytic and computational investigations, as well as simplify understanding and fabrication. More importantly, the simplifications in the test-bed design do not eliminate the complex behavior found in aircraft.

The primary aim of the test-bed will be to experimentally determine techniques for active feedback interior noise control. The design of the control system will involve determining appropriate control algorithms and architectures. Control design will also be heavily dependent on determining actuator and sensor placement. These designs will be based on state-space models derived from the finite element and Rayleigh-Ritz models. Some of the foreseen obstacles include applying control in a computationally feasible manner, designing a controller that minimizes structural vibration as well as interior acoustic noise, and integrating control devices in the structure.

ACKNOWLEDGMENTS

This work was supported by the U.S. Army Research Office under contract number DAAH04-95-1-0104, monitored by Gary Anderson, and by a National Science Foundation graduate fellowship awarded to Donald O'Sullivan. The authors would also like to thank the assistance of Elaine Chen who started the cylinder finite element model.

REFERENCES

1 Clark R.L., M.R. Flemming, and C.R. Fuller, "Piezoelectric Actuators for Distributed Vibration Actuation of thin Plates: A Comparison Between Theory and Experiment," *Journal of Vibration and Acoustics*, July 1993, Vol. 115, pp. 332-339.

2 Hagood N.W., W.H. Chung, and A. von Flotow, "Modelling of Piezoelectric Actuator Dynamics for Active Structural Control," J. of Intell. Mater. Syst. and Struct., Vol. 1, July 1990, pp. 327-354.

3 Baumann W.T., Fu-Sheng Ho, and H.H. Robertshaw, "Active structural acoustic control of broadband disturbances," *Journal of the Acoustical Society of America*, 1992, pp. 1998-2005.

4 Hansen C.H. and S.D. Snyder, "Effect of Geometric and Structural/Acoustic Variables on the Active Control of Sound Radiation from a Vibrating Surface", *Recent Advances in Active Control of Sound and Vibration*, 1991, pp.487-505.

5 Fuller C.R., S.D. Snyder, C.H. Hansen, and R.J. Silcox, "Active Control of Interior Noise in Model Aircraft Fuselages Using Piezoceramic Actuators," *AIAA Journal*, Vol. 30, No. 11, November 1992, pg 2613-2617

6 Dickey J. and G. Maidanik, "Active Control of Response of Ribbed Panels," *Recent Advances in Active Control of Sound and Vibration*, 1991, pp.525-533.

7 Jackson A.C., F.J. Balena, W.L. LaBarge, G. Pei, W.A. Pitman, and G. Wittlin, "Transport Composite Fuselage Technology - Impact Dynamics and Acoustic Transmission," NASA Contractor Report 4035, October 1986.

8 Rossetti D.J. and M.A. Norris, "A Comparison of Actuation and Sensing Techniques for Aircraft Cabin Noise Control," *1994 AIAA Aeroacoustics Conference*, AIAA Paper No. 94-1738.

9 Cabell R.H., H.C. Lester, G.P. Mathur, and B.N. Tran, "Optimization of Actuator Arrays for Aircraft Interior Noise Control," *1993 AIAA Aeroacoustics Conference*, AIAA Paper No. 93-4447.

10 Mathur G.P. and B.N. Tran, "Aircraft Cabin Noise Reduction Tests Using Active Structural Acoustic Control," *1993 AIAA Aeroacoustics Conference*, AIAA Paper No. 93-4437.

11 Simpson M. and B. Tran, "Aircraft Cabin Active Noise Control Performance Sensitivity Tests," *1993 AIAA Aeroacoustics Conference*, AIAA Paper No. 93-4436.

12 MacMartin D.G., G.L. Basso, and B. Leigh, "Noise Transmission and Reduction in Turboprop Aircraft," *78th AGARD Meeting,* May 1994, pp. 21-1 - 21-9.

13 Simpson M.A., P.M. Druez, A.J. Kimbrough, M.P. Brock, P.L. Burgé, G.P. Mathur, M.R. Cannon, and B.N. Tran, "UHB Demonstrator Interior Noise Control Flight Tests and Analysis," NASA Contractor Report 181897, October 1989.

14 Moreland S., *US Army Working Group on Aircraft Noise.*

15 Niesel G. and E. Laudien, "Helicopter Internal Noise," *78th AGARD Meeting,* May 1994, pp. 2-1 - 2-11.

16 How J.P. and S.R. Hall, *Local Control Design Methodologies for a Hierarchic Control Architecture,* Masters Thesis, Massachusetts Institute of Technology, Department of Aeronautics and Astronautics, (Space Systems Laboratory Report #5-90), June 1990.

17 Young K.D., "A Hierarchical Approach to Large Space Structure Control", Dynamics of Flexible Structures in Space - 1st International Conference, May 1990, pp. 183-196.

18 Bernstein D.S. and D.C. Hyland, "Optimal Projection for Uncertain Systems (OPUS): A Unified Theory of Reduced-Order, Robust Control Design", *Large Space Structures: Dynamics and Control*, 1988, pp. 263-302.

19 Hovd M. and S. Skogestad, "Sequential Design of Decentralized Controllers", *Automatica*, 1994, Vol. 30, No. 10, pp. 1601-1607.

20 Weems D., Boeing Helicopter, Personal communcations, Summer 1996.

21 Yoerkie C.A. andP.J. Gintoli, "Development of Rotorcraft Interior Noise Control Concepts, Phase II: Full Scale Testing," NASA Contractor Report 172594, February 1988.

22 Simpson M.A., G.P. Mathur, M.R. Cannon, B.N. Tran, and P.L. Burge, "Fuselage Shell and Cavity Response Measurements on a DC-9 Test Section," NASA Contractor Report 187557, August 1991.

23 MacMartin D.G., United Technologies Research Center, Personal correspondance, June 1996.

24 Blevins R.D, *Formulas for Natural Frequency and Mode Shapes*, Krieger Publishing Company, Malabar,FL, 1995.

25 Flügge W., *Stresses in Shells*, Springer-Verlag, New York, 1973.

26 Kohnke P., "ANSYS User's Manual, Theory," Swanson Analysis Systems, Inc., Houston, PA, December 1992.

27 Flanigan C.C., "Test/Analysis Correlation Using Design Sensitivity and Optimization." *Proceedings of SAE*, Long Beach, CA, Paper #871743 October 1987.

Further author information:
E-mail: nwhagood@mit.edu; WWW: http://web.mit.edu/amsl/; Phone: 617-253-2738; FAX: 617-258-8336